Conformal Data and Renormalization Group Flow in Critical Quantum Spin Chains Using Periodic Uniform Matrix Product States

Yijian Zou,[1,2,*] Ashley Milsted,[1,†] and Guifre Vidal[1]
[1]*Perimeter Institute for Theoretical Physics, Waterloo, Ontario N2L 2Y5, Canada*
[2]*University of Waterloo, Waterloo, Ontario N2L 3G1, Canada*

(Received 22 January 2018; revised manuscript received 8 August 2018; published 7 December 2018)

We establish that a Bloch-state ansatz based on periodic uniform matrix product states (PUMPS), originally designed to capture single-quasiparticle excitations in gapped systems, is in fact capable of accurately approximating all low-energy eigenstates of critical quantum spin chains on the circle. When combined with the methods of [Milsted and Vidal, Phys. Rev. B **96**, 245105] based on the Koo-Saleur formula, PUMPS Bloch states can then be used to identify each low-energy eigenstate of a chain made of up to hundreds of spins with its corresponding scaling operator in the emergent conformal field theory (CFT). This enables the following two tasks that we demonstrate using the quantum Ising model and a recently proposed generalization thereof due to O'Brien and Fendley [Phys. Rev. Lett. 120, 206403]. (i) From the spectrum of low energies and momenta we extract conformal data (specifying the emergent CFT) with unprecedented numerical accuracy. (ii) By changing the lattice size, we investigate nonperturbatively the renormalization group flow of the low-energy spectrum between two CFTs. In our example, where the flow is from the tricritical Ising CFT to the Ising CFT, we obtain excellent agreement with an analytical result [Klassen and Melzer, Nucl. Phys. **B370**, 511] conjectured to describe the flow of the first spectral gap directly in the continuum.

DOI: 10.1103/PhysRevLett.121.230402

Near a continuous phase transition, two microscopically different systems are assigned to the same universality class if they display similar long-distance behavior [1]. In the language of the renormalization group (RG), which describes how physics changes with scale, such systems are said to "flow" to the same scale-invariant theory or RG fixed point. These fixed points are often described by a conformal field theory (CFT) [2,3], which itself is specified by a set of parameters known as conformal data.

Given a microscopic description of a critical system (e.g., a lattice Hamiltonian), an important, yet challenging, task is to extract the conformal data as a means of identifying the universality class of the phase transition. For critical quantum spin chains—the focus of this Letter—much progress can be made in highly fine-tuned models, such as integrable lattice models (e.g., Refs. [4–10]). However, for a generic critical spin chain Hamiltonian, one must resort to numerical methods. Exact diagonalization techniques are certainly useful [11,12], but can only address small systems, where the universal low-energy physics is often concealed by the nonuniversal, microscopic details. Monte Carlo methods can address much larger systems [13], but only in models that do not suffer from the sign problem. On the other hand, tensor network methods [14–16] are both sign-problem free and scalable, and several schemes have been proposed to extract conformal data [17–22]. These include schemes [17–19,21] based on the matrix product state (MPS) [15,23], which is the ansatz underlying the density matrix renormalization group (DMRG) algorithm [14,24].

In this Letter, we establish that a Bloch-state ansatz [25] based on periodic uniform matrix product states (PUMPS) [26] is ideally suited to numerically investigate the emergent universal properties of critical quantum spin chains (see Ref. [27] for previous use in critical systems). Our key observation is that, despite being originally designed to capture only some (namely single-quasiparticle) low-energy excitations in *gapped* systems [25], PUMPS Bloch states turn out to accurately reproduce all low-energy eigenstates of *critical* quantum spin chains (that is, up to some appropriate maximum energy) [28]. The ability of PUMPS to simulate systems consisting of several hundreds of spins allow us to then put forward two new applications of this tensor network ansatz: (i) extraction, with unprecedented accuracy, of the conformal data characterizing the underlying CFT and thus the universality class of the corresponding continuous phase transition; (ii) nonperturbative computation of the RG flow of the low-energy spectrum between two CFTs. Here we demonstrate these applications using the quantum Ising model and its recently proposed generalization due to O'Brien and Fendley [30], with which we study the spectral RG flow between the tricritical Ising CFT and the Ising CFT. We find excellent agreement between our numerical results and an analytical result [31] conjectured to describe the flow of the first spectral gap directly in the continuum.

Matrix product state ansatz.—Given a local Hamiltonian H for a critical quantum spin chain of N spins on the circle, we compute approximations to the ground state and excited states. For the ground state we use a PUMPS $|\Psi(A)\rangle$ [26], which is specified by a tensor A^s_{ab} of dimension $d \times D \times D$, where d is the dimension of the Hilbert space of one spin and D is the *bond dimension*, which restricts the amount of *entanglement*. It has the translation-invariant form $|\Psi(A)\rangle \equiv \sum_{\vec{s}=1}^{d} \mathrm{tr}(A^{s_1}A^{s_2}\ldots A^{s_N})|\vec{s}\rangle$, where $\vec{s} = s_1 \ldots s_N$. To find the variational ground state, we minimize the energy with respect to A^s_{ab} using a gradient descent method [29,32]. We then seek excitations within the space of PUMPS Bloch states [25,27], which have the form

$$|\Phi_p(B)\rangle \equiv \sum_{j=1}^{N} e^{-ipj}\mathcal{T}^j \sum_{\vec{s}=1}^{d} \mathrm{tr}(B^{s_1}A^{s_2},\ldots,A^{s_N})|\vec{s}\rangle, \quad (1)$$

where $\mathcal{T}$ is the translation operator, p is the momentum, A is the ground-state PUMPS tensor, and B^s_{ab} is a tensor that parametrizes a Bloch state and is obtained by diagonalizing an effective Hamiltonian [33].

We assess the performance of the ansatz [Eq. (1)] for critical systems using the critical transverse field Ising model $H = -\sum_{j=1}^{N} [\sigma^X_j \sigma^X_{j+1} + \sigma^Z_j]$. As a first test, we compute the variational ground state and excitations $|\phi_\alpha\rangle$ for a small system of $N = 20$ spins and check the fidelity $f_\alpha \equiv \langle\phi_\alpha|\phi^{\mathrm{exact}}_\alpha\rangle$ with their counterparts computed using exact diagonalization. We find, for the fixed bond dimension $D = 12$, that the first 41 excited states have errors $\epsilon_\alpha \equiv 1 - |f_\alpha|^2$ ranging from 10^{-4} to 10^{-11}, and that this error always scales to zero with increasing D. To test larger systems, where we can no longer use exact diagonalization, we compare the low-energy spectrum of excitation energies with the CFT prediction for the $N \to \infty$ limit. We find that all variational low-energy excitations have energies consistent with the CFT prediction up to a maximum energy that depends on the system size N and the bond dimension D, see Ref. [29] for more details. We conclude that all low-energy excitations are well approximated by the Bloch-state PUMPS [Eq. (1)]. This is remarkable, given that this ansatz was originally proposed [25] for single-quasiparticle excitations in gapped systems, where multiquasiparticle excitations require an alternative, significantly more sophisticated ansatz [41].

Extracting conformal data.—Given the excited states of the critical spin chain, we wish to extract conformal data of the 2D CFT describing its RG fixed point. This includes the *central charge* c and the *scaling dimensions* Δ_α and *conformal spins* S_α of a subset of *scaling operators* ϕ_α (CFT operators that are covariant under dilations and rotations), namely those known as *primary fields* [2]. There are several useful results [42–49] that relate quantities computed from a finite spin chain to this conformal data. Here we make use of the discovery [42–45] that the eigenstates of H have energies E_α and momenta P_α given by

$$E_\alpha = A + B\frac{2\pi}{N}\left(\Delta_\alpha - \frac{c}{12}\right) + O(N^{-x}),$$
$$P_\alpha = \frac{2\pi}{N}S_\alpha, \quad (2)$$

where N is the number of spins, and A, B, x are constants specific to the microscopic model H, with $x > 1$ determining subleading corrections to the dominant scaling with N. Up to these constants, Eq. (2) is determined by universal quantities, with each pair Δ_α, S_α corresponding to a CFT scaling operator ϕ_α via the *operator-state correspondence* [2]. Indeed, we can identify each eigenstate $|\phi_\alpha\rangle$ with a CFT operator ϕ_α using the methods of Ref. [12] based on approximate lattice representations [46]

$$H_n = \frac{N}{2\pi}\sum_{j=1}^{N} e^{ijn(2\pi/N)}h_j \sim L_n + \bar{L}_{-n}, \quad (3)$$

of the Virasoro generators $L_n, \bar{L}_n$ of conformal transformations [2]. These act as *ladder operators* on the eigenstates $|\phi_\alpha\rangle$ of H, which are organized into *conformal towers* of states, each descended from a distinct primary field state. To illustrate how the above identification $|\phi_\alpha\rangle \sim \phi_\alpha$ works, here are three examples: (i) lattice energy eigenstates corresponding to CFT primary operators are those that can not be lowered in energy by any of $H_{\pm1}$, $H_{\pm2}$ (up to some matrix elements that decay with system size) [12]. For instance, in a unitary CFT, the ground state of the critical spin chain is always identified with the primary identity operator I [2]; hence it receives the label $|I\rangle$. (ii) The lattice state $|T\rangle$ corresponding to the stress tensor operator T [2] is characterized as the energy eigenstate $|\psi\rangle$, which maximizes $|\langle\psi|H_{-2}|I\rangle|$, in analogy with the CFT relation $L_{-2}|I\rangle_{\mathrm{CFT}} = \sqrt{(c/2)}|T\rangle_{\mathrm{CFT}}$. Below we use eigenstates $|I\rangle$ and $|T\rangle$ to compute an estimate of the central charge $c \approx 2|\langle T|H_{-2}|I\rangle|^2$ [46]. (iii) The CFT analog of $H_2H_{-2}|I\rangle$ is $(L_2 + \bar{L}_{-2})L_{-2}|I\rangle_{\mathrm{CFT}} = a|I\rangle_{\mathrm{CFT}} + b|T\bar{T}\rangle_{\mathrm{CFT}}$, where a and b are constants of order 1 determined by conformal symmetry, and we have used $\bar{L}_2|I\rangle_{\mathrm{CFT}} = 0$. We may thus identify the lattice state $|T\bar{T}\rangle$ corresponding to the operator $T\bar{T}$ [50–52] as the energy eigenstate $|\psi\rangle \neq |I\rangle$ that maximizes $|\langle\psi|H_2H_{-2}|I\rangle|$.

For instance, for $N = 64$ spins and bond dimension $D = 24$, we obtain a correct identification of all low-energy states $|\phi_\alpha\rangle$ of the critical Ising model with scaling operators ϕ_α of the Ising CFT up to scaling dimension $\Delta_\alpha = 6$ (see Ref. [29] for plots). We then compute variational excitations for a number of system sizes N and, by extrapolating to large N, we estimate the scaling dimensions of a selection of scaling operators, as well as the central charge using Eq. (3): see Table I. We obtain excellent accuracy, with our results being consistently better than those from other methods [20,21,53,54], such as finite-entanglement scaling with infinite MPS [21], or MERA and TNR techniques [20,53] (see Ref. [29] for a detailed

TABLE I. Central charge and selected scaling dimensions from lattice Virasoro matrix elements [12] and energy gaps derived from PUMPS Bloch states [29]. For the Ising model, we used system sizes $N \leq 228$ and bond dimensions $24 \leq D \leq 49$. For the OF model near its tricritical Ising (TCI) point, we used $N \leq 128$ and $28 \leq D \leq 44$ (requiring more computational time than used for the Ising model [29]). Note the good agreement in the latter case, despite being slightly off critical.

Critical Ising model			
	Exact	PUMPS	Error
c	0.5	0.499 9997	10^{-7}
Δ_σ	0.125	0.124 9995	10^{-7}
Δ_ε	1	0.999 9994	10^{-7}
$\Delta_{\partial\bar{\partial}\sigma}$	2.125	2.125 01	10^{-5}
$\Delta_{\partial\bar{\partial}\varepsilon}$	3	3.000 02	10^{-5}
$\Delta_{T\bar{T}}$	4	4.007	10^{-3}

OF model, TCI point			
	Exact	PUMPS	Error
c	0.7	0.6991	10^{-4}
Δ_σ	0.075	0.074 92	10^{-5}
Δ_ε	0.2	0.200 1	10^{-4}
$\Delta_{\sigma'}$	0.875	0.874 7	10^{-4}
$\Delta_{\varepsilon'}$	1.2	1.203	10^{-3}
$\Delta_{\varepsilon''}$	3.0	3.002	10^{-3}

comparison). The computations for this test were carried out in a matter of minutes on a modestly powerful laptop. In addition, the algorithms we use, despite being somewhat more complicated than DMRG, are significantly simpler than those required for the aforementioned methods.

Spectral RG flow.—We now turn [55] to the O'Brien-Fendley (OF) model [30],

$$H = \sum_{j=1}^{N} [-\sigma_j^Z \sigma_{j+1}^Z - \sigma_j^X + \lambda(\sigma_j^X \sigma_{j+1}^Z \sigma_{j+2}^Z + \sigma_j^Z \sigma_{j+1}^Z \sigma_{j+2}^X)], \tag{4}$$

which contains the critical Ising model for $\lambda = 0$ and, as the latter, is symmetric under $\sigma^Z \to -\sigma^Z$ and self-dual under the Kramers-Wannier duality. The model remains in the Ising CFT universality class for $0 \leq \lambda < \lambda_{\mathrm{TCI}}$. At $\lambda_{\mathrm{TCI}} \approx 0.428$ there is a tricritical Ising (TCI) point [30], which we confirm by extracting the central charge and some selected scaling dimensions, shown in Table I, as we did for the Ising model. This model is particularly interesting for our purposes because, with respect to the Ising CFT, the dominant contribution to the λ term comes from the irrelevant $T\bar{T}$ operator [50–52]. With respect to the TCI CFT, the same term corresponds instead to the relevant primary operator ε' ($\phi_{1,3}$ in the Kac table [3]), which is known to generate a flow to the Ising CFT [59,60]. This can be confirmed by computing the matrix elements of the λ term in the low-energy eigenbasis of H at the Ising and TCI points. The interpolating flow between the TCI and the Ising CFTs via closely related operators has been studied in integrable field theory [31,61,62] and in integrable lattice models [5,6,63], as well as using the truncated CFT Hilbert space approach [64,65]. Here, we study the flow nonperturbatively in a nonintegrable lattice model using methods that can be applied to any spin-chain system. To do this, we compute the low-energy spectrum of the model for fixed λ, scaled and shifted so that the ground state has $E = \Delta_I = 0$ and $|T\rangle$ has $E = \Delta_T = 2$ (see Ref. [12]), as a function of the system size N.

We call the flow with N a spectral RG flow [66] to emphasize that we are studying the flow of the low-energy spectrum, rather than the couplings of an effective Hamiltonian. How should we expect the spectral RG flow to look? We can think of the model with $\lambda = \lambda_{\mathrm{TCI}} - \delta$ (for small $\delta > 0$) as a relevant deformation of the TCI CFT. Accordingly, at small N the low-energy physics will be dominated by the nearby TCI point, while increasing N will eventually reveal the Ising CFT. We observe this flow at, e.g., $\lambda = 0.4$, where in Fig. 1 we see that the low-energy excitations spectrum at $N = 32$ exhibits some striking similarities to the TCI CFT spectrum, while at $N = 256$ it looks like the Ising CFT spectrum. Also in Fig. 1, we show conformal tower membership computed using Eq. (3) [12,29]. At $N = 32$, despite strong corrections due to the relevant ε' perturbation and further irrelevant perturbations,

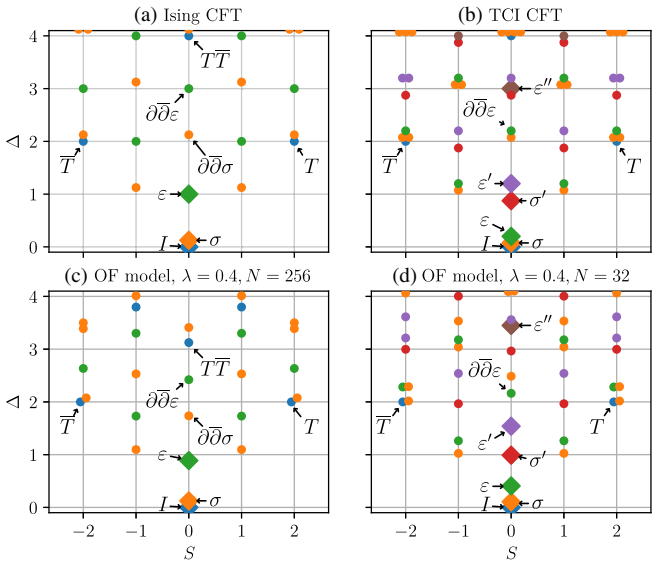

FIG. 1. Top: Scaling operator spectra of (a) the Ising and (b) the TCI CFTs (with a selection of operators labeled). Bottom: Approximate scaling dimensions and conformal-tower identification for the OF model at $\lambda = 0.4$ with (c) $N = 256$, $D = 52$, and (d) $N = 32$, $D = 32$, corresponding to points of Fig. 2. We label a selection of states according to a numerical identification of the corresponding CFT operators [12,29]. Note: We displace data points slightly along the x axis to show degeneracies.

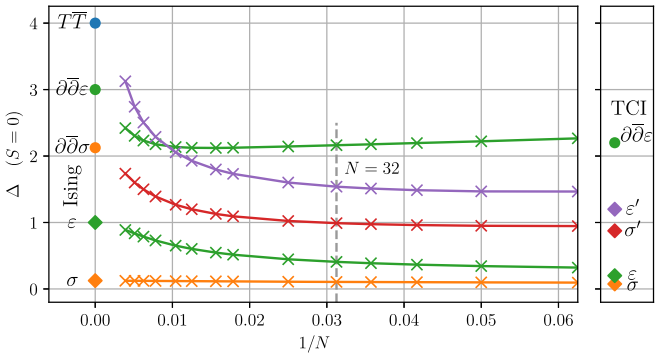

FIG. 2. Spectral RG flow (crosses) of the first five energy levels (as apparent scaling dimensions Δ) at momentum zero, excluding $\Delta = 0$, extracted from the OF model with $\lambda = 0.4$, using PUMPS with $D \leq 52$. For comparison, we also plot the exact scaling dimensions of the Ising and TCI CFTs (dots, diamonds). The crossover between the two highest levels plotted, which we confirm by tracking conformal tower membership using H_n matrix elements, is consistent with these states belonging to different Kramers-Wannier self-duality sectors.

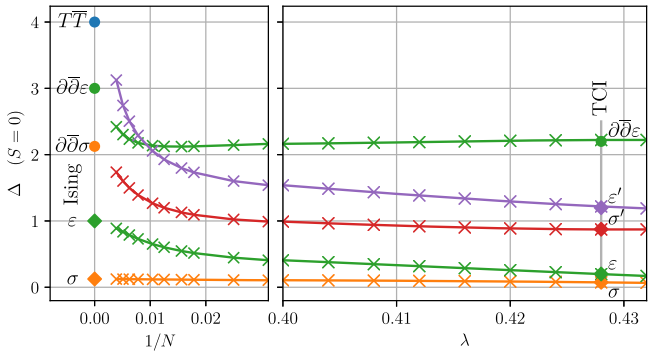

FIG. 3. Connection of the spectral RG flow of Fig. 2 (left) to the "flow" of OF model energy levels as a function of λ at fixed system size $N = 32$, computed using PUMPS with $D = 28$. Note how the apparent scaling dimensions agree with the TCI CFT values at the TCI point $\lambda_{\mathrm{TCI}} \approx 0.428$.

we nevertheless reproduce the low-lying tower-membership results of the TCI. At a large N, the state identifications match the Ising CFT.

In Fig. 2 we further plot the spectral RG flow at $\lambda = 0.4$ for a selection of states, including some that would correspond to primary operators in the TCI CFT. We find we can easily determine which Ising CFT operators the TCI CFT primaries are mapped to:

TCI operator	I	σ	ε	σ'	ε'
Ising operator	I	σ	ε	$\partial\bar{\partial}\sigma$	$T\bar{T}$

These results match those found in other studies of different microscopic realizations of the same CFTs, e.g., Ref. [6], and conform with expectations from symmetry considerations. The identity of ε' in the TCI CFT with $T\bar{T}$ in the Ising CFT matches their both being associated with the λ term in H.

We can better confirm the TCI operator identities of the low-energy states at $\lambda = 0.4$ by tracking them as a function of $\lambda \to \lambda_{\mathrm{TCI}}$. This we do in Fig. 3 for fixed $N = 32$. We find a very similar pattern to Fig. 2, which we would expect if the RG flow of Hamiltonian couplings sends λ to zero for any starting $\lambda < \lambda_{\mathrm{TCI}}$. Using both plots we can connect the low-energy eigenstates at $\lambda = 0.4$, $N = 256$, which we identified with Ising CFT operators, with corresponding eigenstates at λ_{TCI}, $N = 32$, where they clearly match up with TCI CFT operators.

Finally, in Fig. 4, we compare [29] our spectral RG flow to the results of Ref. [31], where methods of integrable field theory are used to arrive at a conjecture for the RG flow of the first spectral gap in the continuum. We find increasingly good agreement for larger system sizes $N \to \infty$, consistent with vanishing finite-size corrections due to lattice effects. We note that our methods should allow us to study nonperturbatively the RG flow of a large number of additional energy levels in generic spin chain systems.

Summary and conclusions.—We have proposed and demonstrated the use of PUMPS and PUMPS Bloch states for extraction of conformal data from critical spin chains. The ability to compute accurate variational low-energy eigenstates at large system sizes (far beyond the reach of exact diagonalization) using these techniques enabled us to study a spectral RG flow in the O'Brien-Fendley model [30] and identify low-energy eigenstates with CFT operators in both the Ising and tricritical Ising CFTs.

We remark that it is *a priori* far from obvious that PUMPS Bloch states should be an appropriate ansatz for all low-energy excited states. After all, in a noncritical spin chain, only single-particle excitations are well captured by this type of ansatz [67], and a different ansatz [41] is needed to capture multiparticle excitations. However, in a critical system (for sufficiently large bond dimension [68]) correlations in the PUMPS are long range so that the tensor B of Eq. (1) is capable of modifying the ground state wave function more globally than in the gapped case, making the ansatz more expressive. Note that the ansatz can easily be

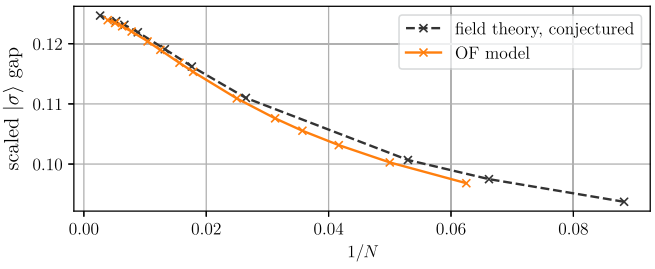

FIG. 4. Flow of the first spectral gap from Fig. 2 compared [29] with the integrable field theory result of Ref. [31], conjectured to describe the equivalent flow in the continuum.

further improved by considering B tensors that encompass two or more lattice sites, instead of one [69].

Finally, we comment on the benefits of dealing with variational energy eigenstates, such as PUMPS Bloch states, that are exact momentum eigenstates by construction. Perhaps most importantly, the momentum directly delivers the conformal spin via Eq. (2), which is therefore known exactly. Furthermore, distinguishing between degenerate energy eigenstates via momentum makes it easier to isolate states corresponding to particular CFT operators. This is crucial for follow-up work [70] in which we variationally determine lattice operators corresponding to CFT primary field operators, allowing us to compute operator product expansion coefficients for primary fields, thus completing the extraction of conformal data from a generic critical quantum spin chain Hamiltonian.

We thank Martin Ganahl for many useful discussions, as well as Jutho Haegeman and Frank Verstraete for valuable comments. We also thank one of the referees for proposing the O'Brien-Fendley model. G. V. thanks the Insitut des Hautes Études Scientifiques (IHES) for hospitality during the workshop "Hamiltonian methods in strongly coupled Quantum Field Theory." The authors acknowledge support from the Simons Foundation (Many Electron Collaboration) and Compute Canada. Research at Perimeter Institute is supported by the Government of Canada through the Department of Innovation, Science and Economic Development Canada and by the Province of Ontario through the Ministry of Research, Innovation and Science.

*yzou@pitp.ca
†amilsted@pitp.ca

[1] K. G. Wilson and J. Kogut, Phys. Rep. **12**, 75 (1974).
[2] A. A. Belavin, A. M. Polyakov, and A. B. Zamolodchikov, Nucl. Phys. **B241**, 333 (1984).
[3] D. Friedan, Z. Qiu, and S. Shenker, Phys. Rev. Lett. **52**, 1575 (1984).
[4] A. B. Zamolodchikov, Nucl. Phys. **B358**, 497 (1991).
[5] G. Feverati, P. A. Pearce, and F. Ravanini, Phys. Lett. B **534**, 216 (2002).
[6] P. A. Pearce, L. Chim, and C. Ahn, Nucl. Phys. **B660**, 579 (2003).
[7] N. Read and H. Saleur, Nucl. Phys. **B777**, 263 (2007).
[8] A. M. Gainutdinov and R. Vasseur, Nucl. Phys. **B868**, 223 (2013).
[9] R. Bondesan, J. Dubail, A. Faribault, and Y. Ikhlef, J. Phys. A **48**, 065205 (2015).
[10] M. S. Zini and Z. Wang, arXiv:1706.08497.
[11] A. Feiguin, S. Trebst, A. W. W. Ludwig, M. Troyer, A. Kitaev, Z. Wang, and M. H. Freedman, Phys. Rev. Lett. **98**, 160409 (2007).
[12] A. Milsted and G. Vidal, Phys. Rev. B **96**, 245105 (2017).
[13] A. W. Sandvik, AIP Conf. Proc. **1297**, 135 (2010).
[14] S. R. White, Phys. Rev. Lett. **69**, 2863 (1992).
[15] M. Fannes, B. Nachtergaele, and R. F. Werner, Commun. Math. Phys. **144**, 443 (1992).
[16] G. Vidal, Phys. Rev. Lett. **99**, 220405 (2007).
[17] C. Degli, E. Boschi, and F. Ortolani, Eur. Phys. J. B **41**, 503 (2004).
[18] L. Tagliacozzo, T. R. de Oliveira, S. Iblisdir, and J. I. Latorre, Phys. Rev. B **78**, 024410 (2008).
[19] J. C. Xavier, Phys. Rev. B **81**, 224404 (2010).
[20] G. Evenbly and G. Vidal, in *Strongly Correlated Systems*, Springer Series in Solid-State Sciences No. 176, edited by A. Avella and F. Mancini (Springer, Berlin Heidelberg, 2013), pp. 99–130.
[21] V. Stojevic, J. Haegeman, I. P. McCulloch, L. Tagliacozzo, and F. Verstraete, Phys. Rev. B **91**, 035120 (2015).
[22] G. Evenbly and G. Vidal, Phys. Rev. Lett. **115**, 180405 (2015).
[23] G. Vidal, Phys. Rev. Lett. **93**, 040502 (2004).
[24] U. Schollwöck, Ann. Phys. (Amsterdam) **326**, 96 (2011).
[25] S. Rommer and S. Östlund, Phys. Rev. B **55**, 2164 (1997).
[26] B. Pirvu, F. Verstraete, and G. Vidal, Phys. Rev. B **83**, 125104 (2011).
[27] B. Pirvu, J. Haegeman, and F. Verstraete, Phys. Rev. B **85**, 035130 (2012).
[28] This observation had been made for two integrable models [26]. We establish its validity for generic critical quantum spin chains via several examples, both integrable and nonintegrable [29].
[29] See Supplemental Material at http://link.aps.org/supplemental/10.1103/PhysRevLett.121.230402 for a detailed description of the algorithm and further numerical results.
[30] E. O'Brien and P. Fendley, Phys. Rev. Lett. **120**, 206403 (2018).
[31] T. R. Klassen and E. Melzer, Nucl. Phys. **B370**, 511 (1992).
[32] M. Ganahl, J. Rincón, and G. Vidal, Phys. Rev. Lett. **118**, 220402 (2017).
[33] For details of the algorithm, see Ref. [29], which includes Refs. [34–40].
[34] G. Vidal, Phys. Rev. Lett. **98**, 070201 (2007).
[35] J. Haegeman, J. I. Cirac, T. J. Osborne, I. Pižorn, H. Verschelde, and F. Verstraete, Phys. Rev. Lett. **107**, 070601 (2011).
[36] F. Verstraete and J. I. Cirac, Phys. Rev. B **73**, 094423 (2006).
[37] F. Verstraete, D. Porras, and J. I. Cirac, Phys. Rev. Lett. **93**, 227205 (2004).
[38] P. Pippan, S. R. White, and H. G. Evertz, Phys. Rev. B **81**, 081103 (2010).
[39] V. Zauner-Stauber, L. Vanderstraeten, M. T. Fishman, F. Verstraete, and J. Haegeman, Phys. Rev. B **97**, 045145 (2018).
[40] I. P. McCulloch, arXiv:0804.2509.
[41] L. Vanderstraeten, F. Verstraete, and J. Haegeman, Phys. Rev. B **92**, 125136 (2015).
[42] J. L. Cardy, J. Phys. A **17**, L385 (1984).
[43] H. W. J. Blöte, J. L. Cardy, and M. P. Nightingale, Phys. Rev. Lett. **56**, 742 (1986).
[44] I. Affleck, Phys. Rev. Lett. **56**, 746 (1986).
[45] J. L. Cardy, Nucl. Phys. **B270**, 186 (1986).
[46] W. M. Koo and H. Saleur, Nucl. Phys. **B426**, 459 (1994).

[47] C. Holzhey, F. Larsen, and F. Wilczek, Nucl. Phys. **B424**, 443 (1994).
[48] P. Calabrese and J. Cardy, J. Stat. Mech. (2004) P06002.
[49] F. C. Alcaraz, M. I. Berganza, and G. Sierra, Phys. Rev. Lett. **106**, 201601 (2011).
[50] L. McGough, M. Mezei, and H. Verlinde, arXiv:1611.03470.
[51] A. Cavaglià, S. Negro, I. M. Szécsényi, and R. Tateo, J. High Energy Phys. 10 (2016) 112.
[52] F. A. Smirnov and A. B. Zamolodchikov, Nucl. Phys. **B915**, 363 (2017).
[53] M. Hauru, G. Evenbly, W. W. Ho, D. Gaiotto, and G. Vidal, Phys. Rev. B **94**, 115125 (2016).
[54] M. Levin and C. P. Nave, Phys. Rev. Lett. **99**, 120601 (2007).
[55] We also studied the closely-related ANNNI model [56–58], results for which we present in Ref. [29].
[56] A. Milsted, L. Seabra, I. C. Fulga, C. W. J. Beenakker, and E. Cobanera, Phys. Rev. B **92**, 085139 (2015).
[57] A. Rahmani, X. Zhu, M. Franz, and I. Affleck, Phys. Rev. B **92**, 235123 (2015).
[58] A. Rahmani, X. Zhu, M. Franz, and I. Affleck, Phys. Rev. Lett. **115**, 166401 (2015).
[59] A. B. Zamolodchikov, Sov. J. Nucl. Phys. **46**, 1090 (1987).
[60] A. W. W. Ludwig and J. L. Cardy, Nucl. Phys. **B285**, 687 (1987).
[61] D. A. Kastor, E. J. Martinec, and S. H. Shenker, Nucl. Phys. **B316**, 590 (1989).
[62] A. B. Zamolodchikov, Nucl. Phys. **B358**, 524 (1991).
[63] G. Feverati and P. Grinza, Nucl. Phys. **B702**, 495 (2004).
[64] M. Lässig, G. Mussardo, and J. L. Cardy, Nucl. Phys. **B348**, 591 (1991).
[65] P. Giokas and G. Watts, arXiv:1106.2448.
[66] Notice that the ratio $1/N$ of the lattice spacing to the system size can be understood as a UV length scale, hence the flow with N can be considered an RG flow.
[67] J. Haegeman, S. Michalakis, B. Nachtergaele, T. J. Osborne, N. Schuch, and F. Verstraete, Phys. Rev. Lett. **111**, 080401 (2013).
[68] B. Pirvu, G. Vidal, F. Verstraete, and L. Tagliacozzo, Phys. Rev. B **86**, 075117 (2012).
[69] J. Haegeman, T. J. Osborne, and F. Verstraete, Phys. Rev. B **88**, 075133 (2013).
[70] Y. Zou, A. Milsted, and G. Vidal (to be published).